

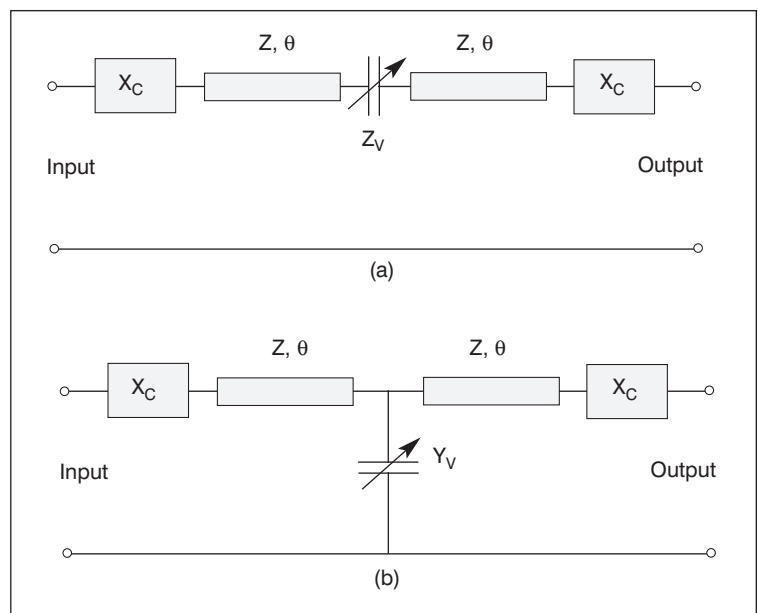
Modeling Varactor Tunable Microstrip Resonators for Wireless Applications

By Boris Kapilevich and Roman Lukyanets
Siberia State Academy of Telecommunications and Informatics

Varactor tunable resonators (VTR) are microwave components rapidly becoming popular for creating both passive and active tunable filters. They have attracted the attention of specialists as an important element in adaptive communication systems. If combined with a proper control circuit, useful and powerful components can be constructed for development of frequency variable equipment such as frequency hopping converters for TDMA communication systems. There have been many different VTR configurations suggested during the past decade. Some of them are considered in [1-4]. But the typical problem inherent in many VTR configurations is degraded Q-factor of a resonator due to insufficient quality of the varactor itself. However, combining such circuits with a negative resistance element is an effective way to improve the situation. Keeping this idea in the mind, this article focuses on VTR configurations which might be easily implemented for microwave active filters (MAF) [5] and their channelized modifications [6].

Basic varactor tuned resonator (VTR) configurations

Various configurations of VTR can be suggested for microwave active filter design. Depending on the number of diodes, both single (Figure 1) and double (Figure 2) terminated circuits can be used, with series or parallel connections within the resonator. Resonance conditions and tuning capabilities of these configurations



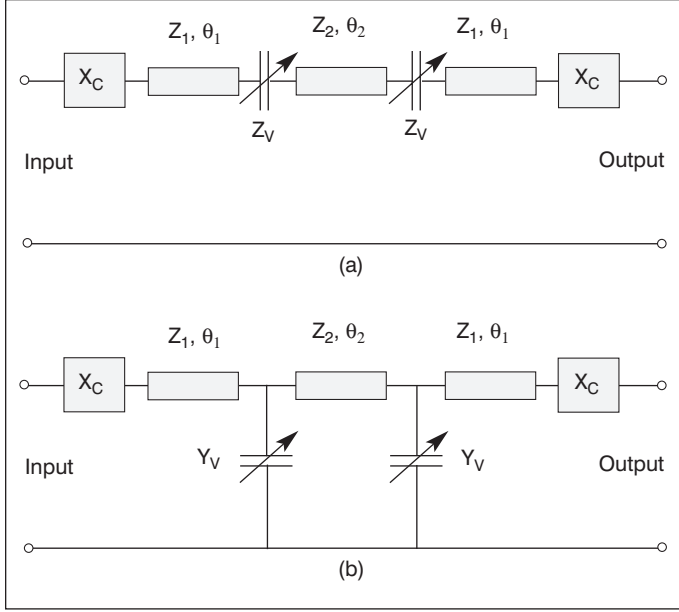
■ Figure 1. Configurations of single terminated varactor tunable resonators: (a) in series, (b) in parallel.

are investigated below on the basis of appropriate circuit models, to determine the best one suitable for microwave active filter design.

VTR using sections of uniform transmission line and a single varactor

Let consider simple VTR configurations with different varactor connections: in series (Figure 1a) and in parallel (Figure 1b). Proper transmission matrices are:

$$[V] = \begin{bmatrix} 1 & Z_V \\ Y_V & 1 \end{bmatrix} \quad (1)$$



■ **Figure 2. Configurations of double terminated varactor tunable resonators: (a) in series, (b) in parallel.**

$$[C] = \begin{bmatrix} 1 & X_C \\ 0 & 1 \end{bmatrix} \quad (2)$$

$$[Tr] = \begin{bmatrix} \cos \theta & iZ \sin \theta \\ \frac{i}{Z} \sin \theta & \cos \theta \end{bmatrix} \quad (3)$$

where:

- $[V]$ is for the varactor;
- $[C]$ is for the coupling input/output elements;
- $[Tr]$ is for a section of uniform transmission line;
- $Z_V = 0$, $Y_V \neq 0$ for parallel connection, $Z_V \neq 0$, $Y_V = 0$ for series connection (Z_V is the varactor impedance and Y_V is a varactor admittance);
- Z is the system impedance;
- l is the length of the section of uniform line;
- $\theta = 2\pi l / \lambda_{\text{eff}}$, where λ_{eff} is effective wavelength;
- X_C is the reactance of the coupling elements at the input/output.

The resultant transmission matrix $[R]$ of a VTR is the product of the above written transmission matrices:

$$[R] = [C] \times [Tr] \times [V] \times [Tr] \times [C] \quad (4)$$

After multiplying matrices in (4) the following expression for elements of the resultant transmission matrix can be written:

$$[R_S] = \begin{bmatrix} A_S & B_S \\ C_S & D_S \end{bmatrix} \quad (5)$$

$$[R_P] = \begin{bmatrix} A_P & B_P \\ C_P & D_P \end{bmatrix} \quad (6)$$

Combining (4) with (1), (2), (3) the following elements of $[R_S]$ can be presented:

$$\begin{aligned} \text{Re}(A_S) &= \cos\left(\frac{1}{2}\theta_2\right)\cos(\theta_1) - \frac{1}{Z_1 Z_2} \sin Z_V X_C \sin(\theta_1) \\ &\quad - \frac{Z_1}{Z_2} \sin\left(\frac{1}{2}\theta_2\right)\sin(\theta_1) \\ \text{Im}(A_S) &= \frac{1}{Z_1} \cos\left(\frac{1}{2}\theta_2\right) X_C \sin(\theta_1) \\ &\quad + \frac{1}{Z_2} \sin\left(\frac{1}{2}\theta_2\right) Z_V \cos(\theta_1) + \frac{1}{Z_2} \sin\left(\frac{1}{2}\theta_2\right) X_C \cos(\theta_1) \quad (7) \end{aligned}$$

$$\begin{aligned} \text{Re}(B_S) &= -\frac{1}{Z_1} Z_2 \sin\left(\frac{1}{2}\theta_2\right) X_C \sin(\theta_1) + \cos\left(\frac{1}{2}\theta_2\right) Z_V \cos(\theta_1) \\ &\quad + \cos\left(\frac{1}{2}\theta_2\right) X_C \cos(\theta_1) \end{aligned}$$

$$\begin{aligned} \text{Im}(B_S) &= Z_2 \sin\left(\frac{1}{2}\theta_2\right) \cos(\theta_1) + \frac{1}{Z_1} \cos\left(\frac{1}{2}\theta_2\right) Z_V X_C \sin(\theta_1) \\ &\quad + Z_1 \cos\left(\frac{1}{2}\theta_2\right) \sin(\theta_1) \end{aligned}$$

$$\text{Re}(C_S) = \sin\left(\frac{1}{2}\theta_2\right) Z_V \frac{\sin(\theta_1)}{Z_1 Z_2}$$

$$D_S = A_S$$

By the same calculations we can get the following elements of $[R_P]$:

$$D_P = A_P$$

$$\text{Re}(A_P) = \cos(\theta)^2 (2 + Y_V X_C) - 1$$

$$\text{Im}(A_P) = \sin(2\theta) \frac{2X_C + Z^2 Y_V}{2Z}$$

$$\text{Re}(B_P) = \cos(\theta)^2 (2X_C + Y_V X_C^2) - (2X_C + Z^2 Y_V) \sin(\theta)^2$$

$$\text{Im}(B_P) = \sin(2\theta) \frac{X_C^2 + Z^2 Y_V X_C + Z^2}{Z} \quad (8)$$

$$\text{Re}(C_P) = \cos(\theta)^2 Y_V$$

$$\text{Im}(C_P) = 2\cos(\theta) \frac{\sin(2\theta)}{Z}$$

Resonance conditions

The above expressions can be used to estimate resonance conditions $|S_{11}| = 0$ which correspond to the

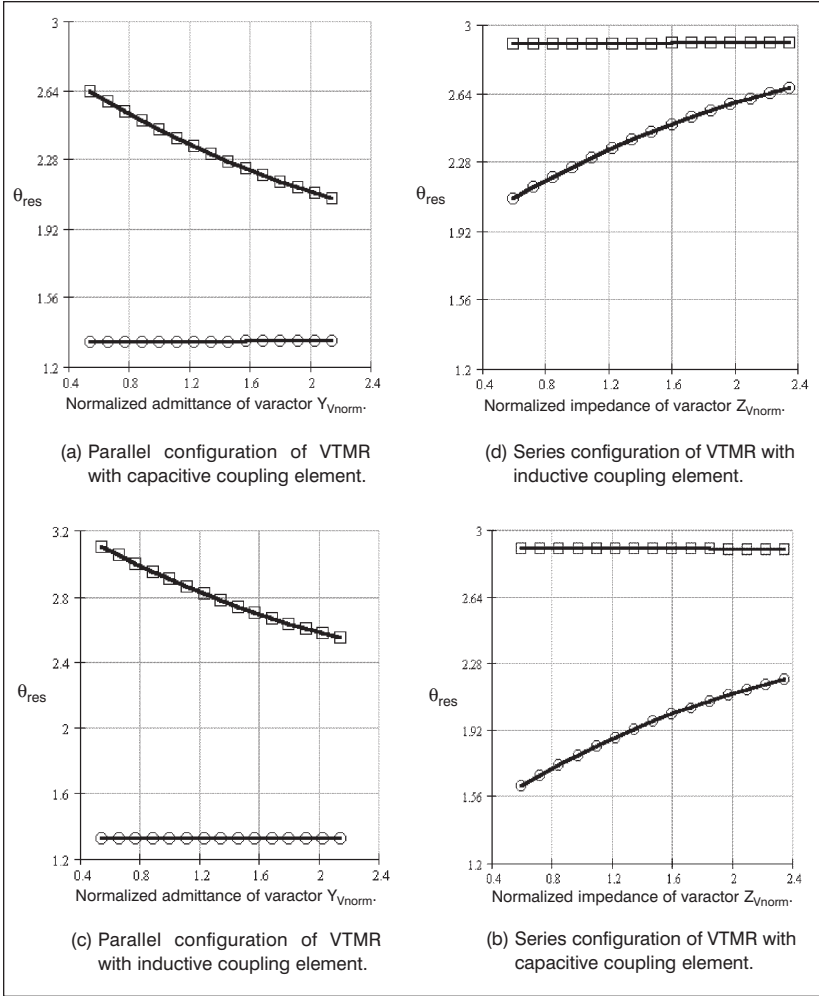


Figure 3. Behavior of the calculated θ_{res} as a function of normalized Z_V and Y_V for different coupling elements. Plots marked with circles are the first resonance, squares are the second resonance.

following equalities:

$$B_S = C_S \quad \text{and} \quad B_P = C_P \quad (9)$$

Substituting (7) and (8) into (9), the common resonance condition determining a resonance length θ_{res} of the VTR can be written:

| Type of Configuration | The type of coupling element | |
|-----------------------|--|---|
| | Capacitor | Inductor |
| In series | $a = -16X_C + 4Z_V \times X_C^2 / Z^2 - 4Z_V + 4Z_V \times Z_0^2 / Z^2$ $b = -2X_C - Z_V$ $d = X_C^2 / Z + Z_V \times X_C / Z - Z + Z_0^2 / Z$ | $a = 16X_C + 4X_C^2 \times Z_V / Z^2 - 4Z_V + 4 \times Z_0^2 \times Z_V / Z^2$ $b = 2X_C - Z_V$ $d = X_C^2 / Z - Z_V \times X_C / Z + Z + Z_0^2 / Z$ |
| In parallel | $a = -16X_C - 4X_C^2 \times Y_V + 4Z^2 \times Y_V - 4Y_V \times Z_0^2$ $b = -2X_C - Z_C^2 \times Y_V - Z_0^2 \times Y_V$ $d = X_C^2 / Z - Z \times X_C \times Y_V - Z + Z_0^2 / Z$ | $a = 16X_C - 4X_C^2 \times Y_V + 4Z^2 Y_V - 4Y_V \times Z_0^2$ $b = 2X_C - Z_C^2 \times Y_V - Y_V \times Z_0^2$ $d = X_C^2 / Z + Z \times X_C \times Y_V - Z + Z_0^2 / Z$ |

Table 1. Expressions for a, b and d coefficients determining a resonance condition of different single varactor terminated configurations.

$$P_1 \times t_4 - P_2 \times t_3 + P_3 \times t_2 - P_4 \times t + P_5 = 0 \quad (10)$$

where $t = \cos^2(\theta/2)$

P_1, P_2, P_3, P_4 and P_5 are the polynomial coefficients depending on the varactor's parameter and the impedance of the coupling element and are calculated as follows:

$$\begin{aligned} P_1 &= a^2 + 64d^2 \\ P_2 &= 2a^2 + 128d^2 \\ P_3 &= a^2 + 2ab + 80d^2 \\ P_4 &= 2ab + 16d^2 \\ P_5 &= b^2 \end{aligned}$$

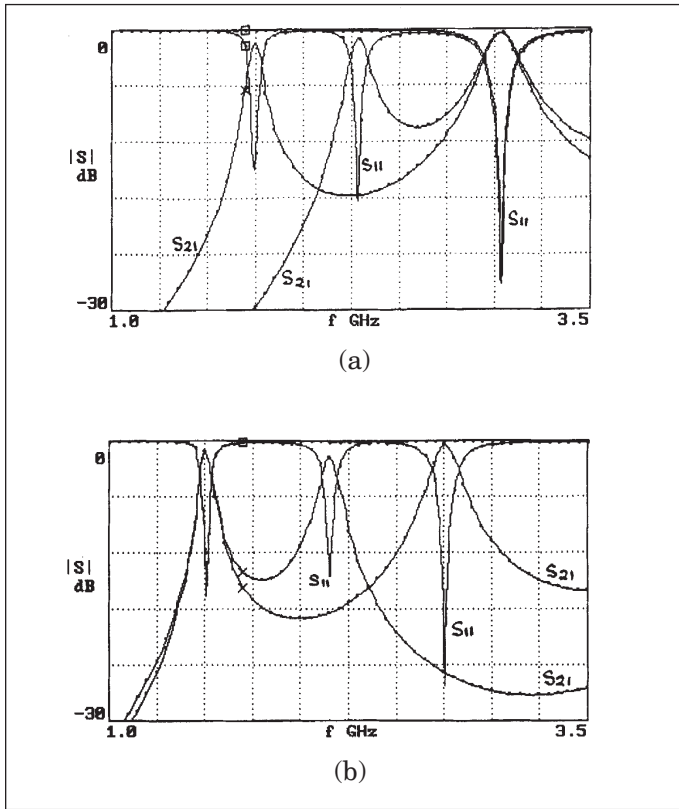
For simplicity, coupling elements such as a capacitor or inductor are discussed below. Each of them provides a specified value of θ_{res} through parameters a, b and d . The expressions for a, b and d determining a resonance condition of the given VTR configuration are presented in Table 1 where Z_0 is the system impedance.

The behavior of the calculated resonant electric lengths θ_{res} are shown in Figure 3 for both series and parallel configurations as a function of normalized varactor impedance Z_V and normalized varactor admittance Y_V . It was assumed that the normalized impedance of coupling capacitor is $C_{norm} = 6$ and normalized impedance of resonator section is 1.5. It should be pointed out that the frequency separation between adjacent resonance modes tends to decrease when impedance (or admittance) is increased. The inductive coupling in series configuration is unfavorable, demonstrating lesser separation between these modes. This phenomenon establishes the physical limit of tuning range for the configurations discussed and filters based on such resonators.

for the configurations discussed and filters based on such resonators.

Both series and parallel configurations exhibit odd and even resonances with different tuning behavior. The lowest resonance is odd and the nearest higher one is even resulting in a maximum current amplitude or maximum voltage amplitude in the center of a resonator, respectively. All odd resonances are tuned and all even ones are fixed in the case of series configuration. The situation is exactly opposite for a parallel one.

The calculated performance of a varactor tunable microstrip resonator (VTMR) is shown in



■ **Figure 4. Amplitude responses of VTMR for series (a) and parallel (b) configurations.**

Figure 4, as a function of a frequency. The following parameters were assumed:

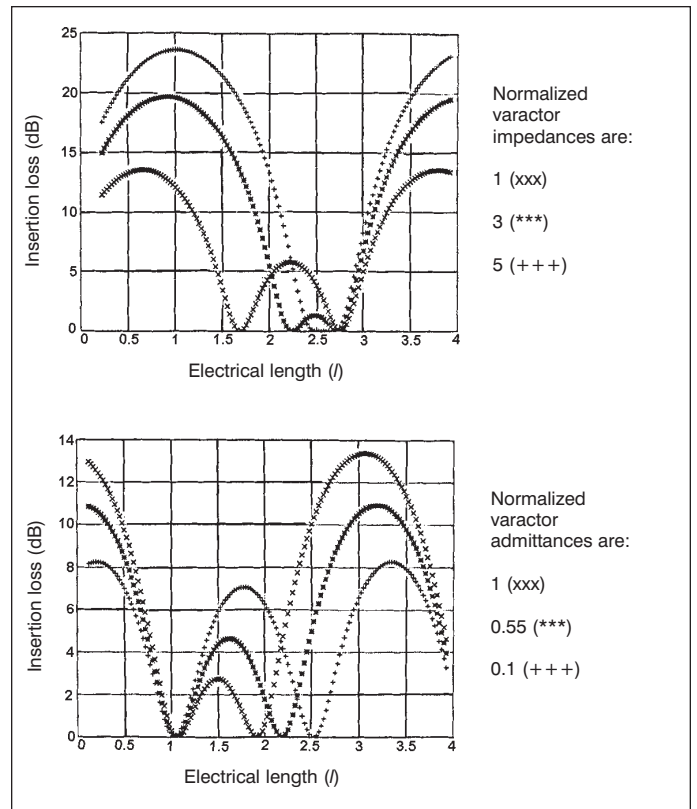
- resonator impedance = 80 ohms, resonator length = 180° , Q factor = 300;
- coupling capacitance = 0.3 pF, varactor capacitances: $C_j(0)=2.5$ pF and $C_j(b)=0.5$ pF;
- substrate is Al_2O_3 , thickness = 1 mm, permittivity = 9.8, system impedance = 50 ohms;
- design frequency = 1.7 GHz.

The tuning range is about 550-600 MHz for both configurations. The next highest resonance is placed near 3 GHz. Since the lowest tuning mode is preferable, the series configuration is recommended in practice.

It should be pointed out that another problem can take place with odd and even resonances moving towards each other. They can produce a two-pole filter, like coupled resonators. Figure 5 illustrates this behavior for both configurations with the normalized impedance of a coupling capacitor $C=2$. In practice, the phenomenon discussed will restrict the available bandwidth of tunable active filters.

VTR using double terminated varactors in series

The analysis of a resonator can be simplified by using its symmetry property with respect to input/output ports. It is very useful for studying double terminated varactors. Hence, a transmission matrix of the



■ **Figure 5. Effects of coupling on different VTMR configurations using capacitive coupling.**

left and right parts of the resonator are dependent on each other, specifically,

$$[A]_{\text{left}} = \begin{bmatrix} A_S & B_S \\ C_S & D_S \end{bmatrix} \quad \text{and} \quad [A]_{\text{right}} = \begin{bmatrix} D_S & B_S \\ C_S & A_S \end{bmatrix} \quad (11)$$

So only the matrix in (11) must be determined, which simplifies the analysis. The matrix $[A]_{\text{left}}$ can be written as follows:

$$[A]_{\text{left}} = [C] \times [Tr_1 \theta_1] \times [V] \times [Tr_2 \theta_2 / 2] \quad (12)$$

where

$$[Tr_1] = \begin{bmatrix} \cos \theta_1 & iZ_1 \sin \theta_1 \\ \frac{i}{Z_1} \sin \theta_1 & \cos \theta_1 \end{bmatrix} \quad (13)$$

$$[Tr_2] = \begin{bmatrix} \cos(\theta_2 / 2) & iZ_2 \sin(\theta_2 / 2) \\ \frac{i}{Z_2} \sin(\theta_2 / 2) & \cos(\theta_2 / 2) \end{bmatrix}$$

Multiplication matrices in (12) yield the following expressions for elements of $[A]_{\text{left}}$:

$$\begin{aligned} \text{Re}(A_S) &= \cos\left(\frac{1}{2}\theta_2\right)\cos(\theta_1) - \frac{1}{Z_1 Z_2} \sin Z_V X_C \sin(\theta_1) \\ &\quad - \frac{Z_1}{Z_2} \sin\left(\frac{1}{2}\theta_2\right)\sin(\theta_1) \end{aligned}$$

$$\begin{aligned} \text{Im}(A_S) &= \frac{1}{Z_1} \cos\left(\frac{1}{2}\theta_2\right) X_C \sin(\theta_1) \\ &\quad + \frac{1}{Z_2} \sin\left(\frac{1}{2}\theta_2\right) Z_V \cos(\theta_1) + \frac{1}{Z_2} \sin\left(\frac{1}{2}\theta_2\right) X_C \cos(\theta_1) \end{aligned}$$

$$\begin{aligned} \text{Re}(B_S) &= -\frac{1}{Z_1} Z_2 \sin\left(\frac{1}{2}\theta_2\right) X_C \sin(\theta_1) + \cos\left(\frac{1}{2}\theta_2\right) Z_V \cos(\theta_1) \\ &\quad + \cos\left(\frac{1}{2}\theta_2\right) X_C \cos(\theta_1) \end{aligned}$$

$$\begin{aligned} \text{Im}(B_S) &= Z_2 \sin\left(\frac{1}{2}\theta_2\right) \cos(\theta_1) + \frac{1}{Z_1} \cos\left(\frac{1}{2}\theta_2\right) Z_V X_C \sin(\theta_1) \\ &\quad + Z_1 \cos\left(\frac{1}{2}\theta_2\right) \sin(\theta_1) \end{aligned} \quad (14)$$

$$\text{Re}(C_S) = \sin\left(\frac{1}{2}\theta_2\right) Z_V \frac{\sin(\theta_1)}{Z_1 Z_2}$$

$$\text{Im}(C_S) = \frac{1}{Z_1} \cos\left(\frac{1}{2}\theta_2\right) \sin(\theta_1) + \frac{1}{Z_2} \sin\left(\frac{1}{2}\theta_2\right) \cos(\theta_1)$$

$$\text{Re}(D_S) = -\frac{1}{Z_1} Z_2 \sin\left(\frac{1}{2}\theta_2\right) \sin(\theta_1) + \cos\left(\frac{1}{2}\theta_2\right) \cos(\theta_1)$$

$$\text{Im}(D_S) = \cos\left(\frac{1}{2}\theta_2\right) Z_V \frac{\sin(\theta_1)}{Z_1}$$

Finally, a resultant transmission matrix of the resonator considered can be written as follows using (11):

$$[R_S] = \begin{bmatrix} A_S D_S + B_S C_S & 2A_S B_S \\ 2C_S D_S & A_S D_S + B_S C_S \end{bmatrix} \quad (15)$$

VTR using double terminated varactors in parallel

Repeating similar calculations for a parallel double terminated varactor configuration and taking into account (11) the case discussed, the following expressions of transmission matrix elements can be written:

$$\begin{aligned} \text{Re}(A_P) &= \cos\left(\frac{1}{2}\theta_2\right)\cos(\theta_1) + \cos\left(\frac{1}{2}\theta_2\right) Y_V Y_C \cos(\theta_1) \\ &\quad + \frac{1}{Z_2} \sin\left(\frac{1}{2}\theta_2\right) Z_1 \sin(\theta_1) \end{aligned}$$

$$\begin{aligned} \text{Im}(A_P) &= \frac{1}{Z_1} \cos\left(\frac{1}{2}\theta_2\right) X_C \sin(\theta_1) + Z_1 \cos\left(\frac{1}{2}\theta_2\right) Y_V \sin(\theta_1) \\ &\quad + \frac{1}{Z_2} \sin\left(\frac{1}{2}\theta_2\right) X_C \cos(\theta_1) \end{aligned}$$

$$\begin{aligned} \text{Re}(B_P) &= -\frac{1}{Z_1} Z_2 \sin\left(\frac{1}{2}\theta_2\right) X_C \sin(\theta_1) \\ &\quad - Z_1 Z_2 \sin\left(\frac{1}{2}\theta_2\right) Y_V \cos(\theta_1) \\ &\quad + \cos\left(\frac{1}{2}\theta_2\right) X_C \cos(\theta_1) \end{aligned}$$

$$\begin{aligned} \text{Im}(B_P) &= Z_2 \sin\left(\frac{1}{2}\theta_2\right) \cos(\theta_1) + Z_2 \sin\left(\frac{1}{2}\theta_2\right) Y_V X_C \cos(\theta_1) \\ &\quad + Z_1 \cos\left(\frac{1}{2}\theta_2\right) \sin(\theta_1) \end{aligned} \quad (16)$$

$$\text{Re}(C_P) = \cos(\theta_2 / 2) Y_V \cos(\theta_1)$$

$$\text{Im}(C_P) = \cos(\theta_2 / 2) \sin(\theta_1) / Z_1 + \sin(\theta_2 / 2) \cos(\theta_1) / Z_2$$

$$\text{Re}(D_P) = -\sin(\theta_2 / 2) \sin(\theta_1) Z_2 / Z_1 + \cos(\theta_2 / 2) \cos(\theta_1)$$

$$\text{Im}(D_P) = \sin(\theta_2 / 2) \cos(\theta_1) Z_2 Y_V$$

Finally, a resultant transmission matrix of the resonator considered can be written in the following form using relationships similar to (15):

$$[R_P] = \begin{bmatrix} A_P D_P + B_P C_P & 2A_P B_P \\ 2C_P D_P & A_P D_P + B_P C_P \end{bmatrix} \quad (17)$$

The resonance conditions can be determined using the same method:

$$A_S B_S - C_S D_S = 0 \text{ for series configuration} \quad (18)$$

$$A_P B_P - C_P D_P = 0 \text{ for parallel configuration} \quad (19)$$

However, their analytic form is rather complicated and omitted here. Instead, examples of VTMR performance are given below.

VTR performance of series and parallel configurations using double terminated varactors.

Based on the above expressions for resultant transmission matrices of series $[R_S]$ and parallel $[R_P]$ configurations, the performance and tuning range of VTMRs can be estimated as a function of circuit topology. For simplicity of comparison, the parameters of VTMRs are assumed to be the same as we have used earlier in Figure 4 as well as the capacitance of the varactor, $C_j = 0.5\text{-}2.5$ pF. Impedance and length of transmission line sections are varied in order to search for the best tuning range. Some typical results are presented in Table 2 and

Table 3 for series and parallel configurations.

Both configurations have demonstrated the existence of “tuned” modes only. This can be explained by shifting varactors to the side of the resonator center. However, their tuning range becomes strongly different. The series configurations have exhibited much better tuning range, between 450 MHz and 1100 MHz (see Table 2 and Figures 6 and 7). The tuning range of parallel configurations is less than that of the series ones, lying between 150 MHz and 360 MHz (see Table 3 and Figures 8 and 9). Hence, the double terminated varactor resonators with a series configuration are preferable for implementation in practice.

If we compare single and double varactor terminated configurations, the latter exhibits much higher tuning range. However, it has a more complicated biasing circuit, increasing the cost with respect to a resonator using a single varactor.

| Z_1, Ω | θ_1, deg | Z_2, Ω | θ_2, deg | $f_{\text{res}}, \text{MHz}$ $C_j = 2.5 \text{ pF}$ | $f_{\text{res}}, \text{MHz}$ $C_j = 0.5 \text{ pF}$ | Tuning range, MHz |
|---------------|------------------------|---------------|------------------------|--|--|----------------------|
| 65 | 45 | 35 | 90 | 2767.7 | 2111.1 | 656.6 |
| 35 | 45 | 65 | 90 | 2464.6 | 1707.1 | 757.5 |
| 35 | 60 | 65 | 60 | 3020.2 | 1909.1 | 1111.1 |
| 35 | 30 | 65 | 120 | 2010.1 | 1555.6 | 454.5 |

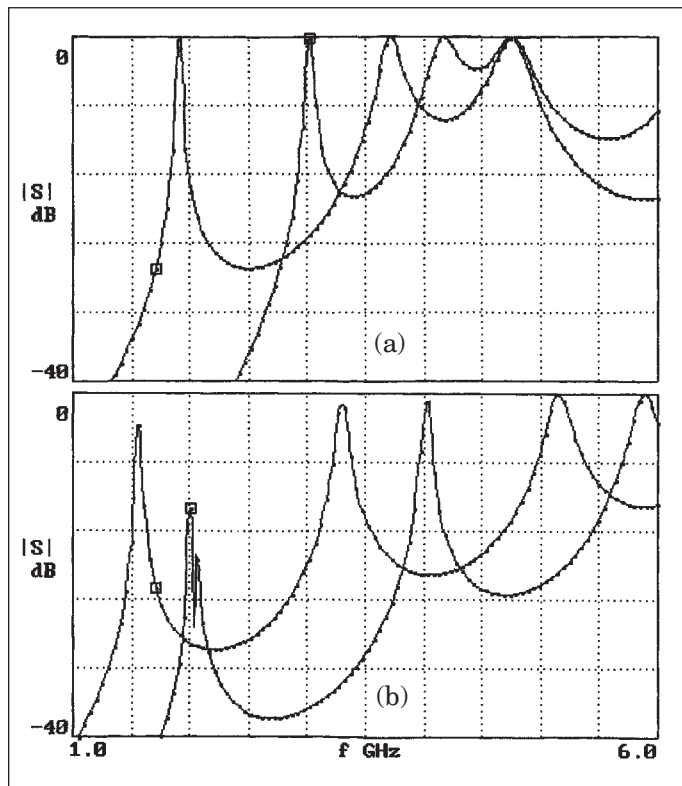
■ **Table 2. Series configuration of double terminated varactors.**

| Z_1, Ω | θ_1, deg | Z_2, Ω | θ_2, deg | $f_{\text{res}}, \text{MHz}$ $C_j = 2.5 \text{ pF}$ | $f_{\text{res}}, \text{MHz}$ $C_j = 0.5 \text{ pF}$ | Tuning range, MHz |
|---------------|------------------------|---------------|------------------------|--|--|----------------------|
| 65 | 45 | 35 | 90 | 1688.4 | 1386.9 | 301.5 |
| 35 | 45 | 65 | 90 | 1206.0 | 964.8 | 241.2 |
| 65 | 60 | 35 | 60 | 1688.4 | 1537.7 | 150.7 |
| 65 | 30 | 35 | 120 | 1628.1 | 1266.3 | 361.8 |

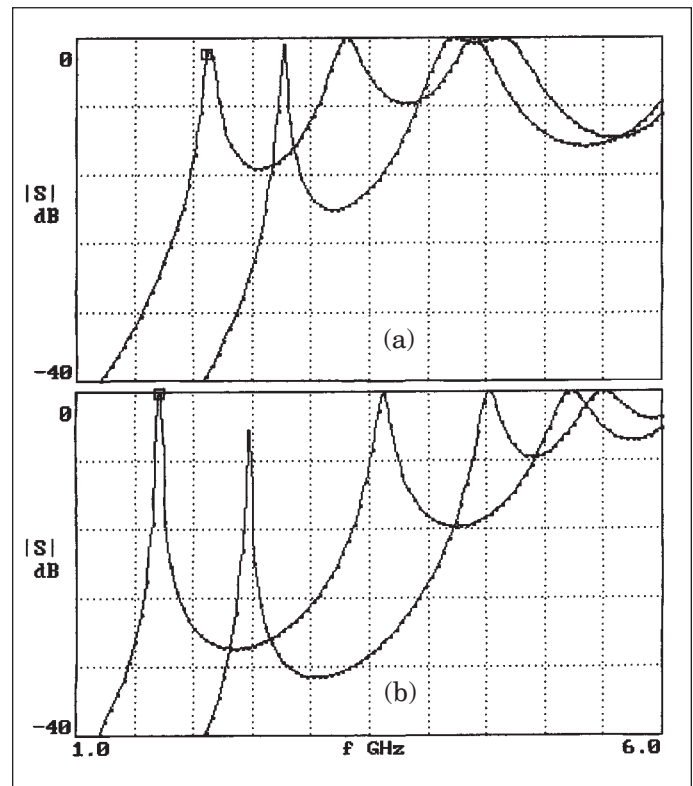
■ **Table 3. Parallel configuration of double terminated varactors.**

Varactor choice

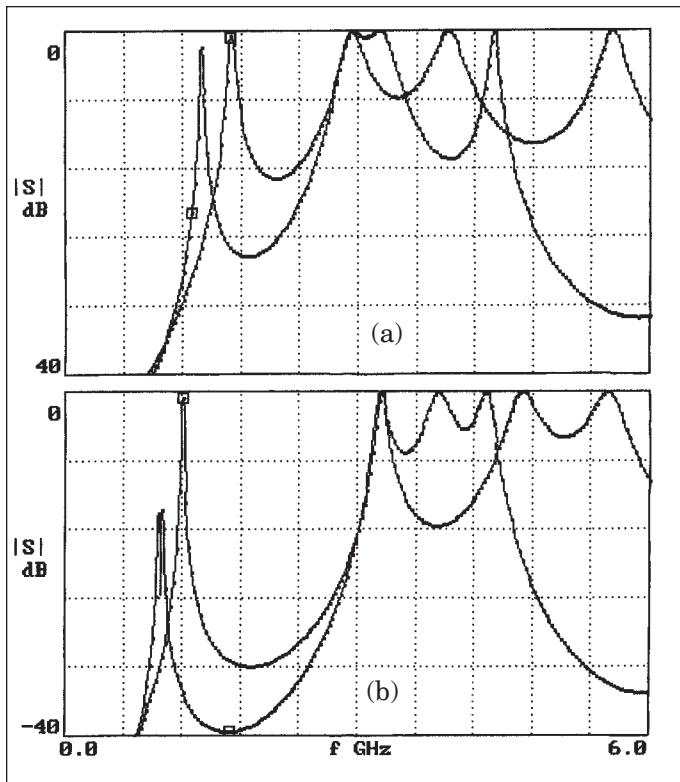
There are many types of microwave varactors commercially available at present. For comparison purposes, three types of varactor were evaluated in the single terminated configurations using capacitive coupling:



■ **Figure 6. VTM performance for various configurations of double terminated varactor diodes in series: (a) $Z_1=35\Omega$, $\theta_1=60^\circ$; $Z_2=65\Omega$, $\theta_2=60^\circ$; (b) $Z_1=35\Omega$, $\theta_1=30^\circ$, $Z_2=65\Omega$, $\theta_2=120^\circ$.**



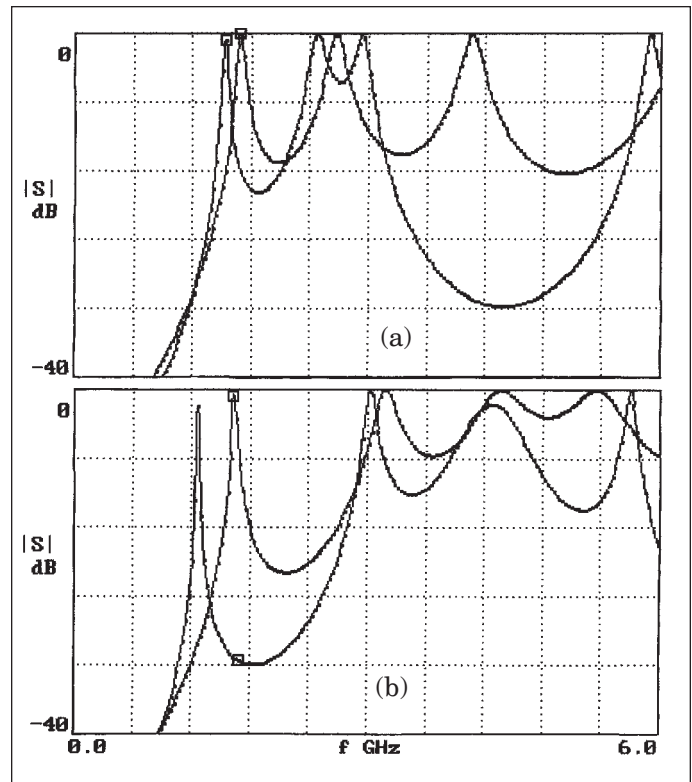
■ **Figure 7. VTM performance for various configurations of double terminated varactor diodes in series: (a) $Z_1=65\Omega$, $\theta_1=45^\circ$; $Z_2=35\Omega$, $\theta_2=90^\circ$; (b) $Z_1=35\Omega$, $\theta_1=45^\circ$, $Z_2=65\Omega$, $\theta_2=90^\circ$.**



■ **Figure 8. VTMR performance for various configurations of double terminated varactor diodes in parallel: (a) $Z_1=65\Omega$, $\theta_1=60^\circ$; $Z_2=35\Omega$, $\theta_2=60^\circ$; (b) $Z_1=65\Omega$, $\theta_1=30^\circ$, $Z_2=35\Omega$, $\theta_2=120^\circ$.**

- An abrupt-junction silicon varactor (epitaxial breakdown voltage of 50 V) with $C_j(0) = 2.4$ pF and $C_j(b) = 0.27$ pF. When connected in the proper series configuration, the VTMR provides a tuning range of 560 MHz as shown in Figure 10(a).
- A varactor similar to the previous one but with capacitance ratio of 6:1 from 0 V to 30 V having $C_j(0) = 1.42$ pF and $C_j(30) = 0.22$ pF. The tuning range of this varactor is less than the first type, specifically 450 MHz, as shown in Figure 10(b). This is due to the lower junction capacitance at zero bias compared to the previous device.
- A Siemens BB801 packaged varactor diode with $C_j(0) = 1$ pF and $C_j(b) = 2$ pF. For this type of varactor, the tuning range is about 250 MHz, as shown in Figure 10(c).

Before calculating the characteristics depicted on Figure 10, scattering parameters of varactors were estimated on the basis of their equivalent circuits [7]. It is obvious that the tuning range is primarily a function of the capacitance ratio of a varactor depending on available varactor voltage limits. Highest cutoff frequencies are always associated with low breakdown voltages. For broadband tuning, a varactor with high cutoff frequen-



■ **Figure 9. VTMR performance for various configurations of double terminated varactor diodes in parallel: (a) $Z_1=65\Omega$, $\theta_1=45^\circ$; $Z_2=35\Omega$, $\theta_2=90^\circ$; (b) $Z_1=35\Omega$, $\theta_1=45^\circ$, $Z_2=65\Omega$, $\theta_2=90^\circ$.**

cy (high-Q) and large capacitance ratio is the most suitable. Observing the performance of the VTMRs considered, the abrupt-junction silicon varactor with breakdown voltage of 50 V demonstrates the best characteristics among the three varactors compared.

Conclusion

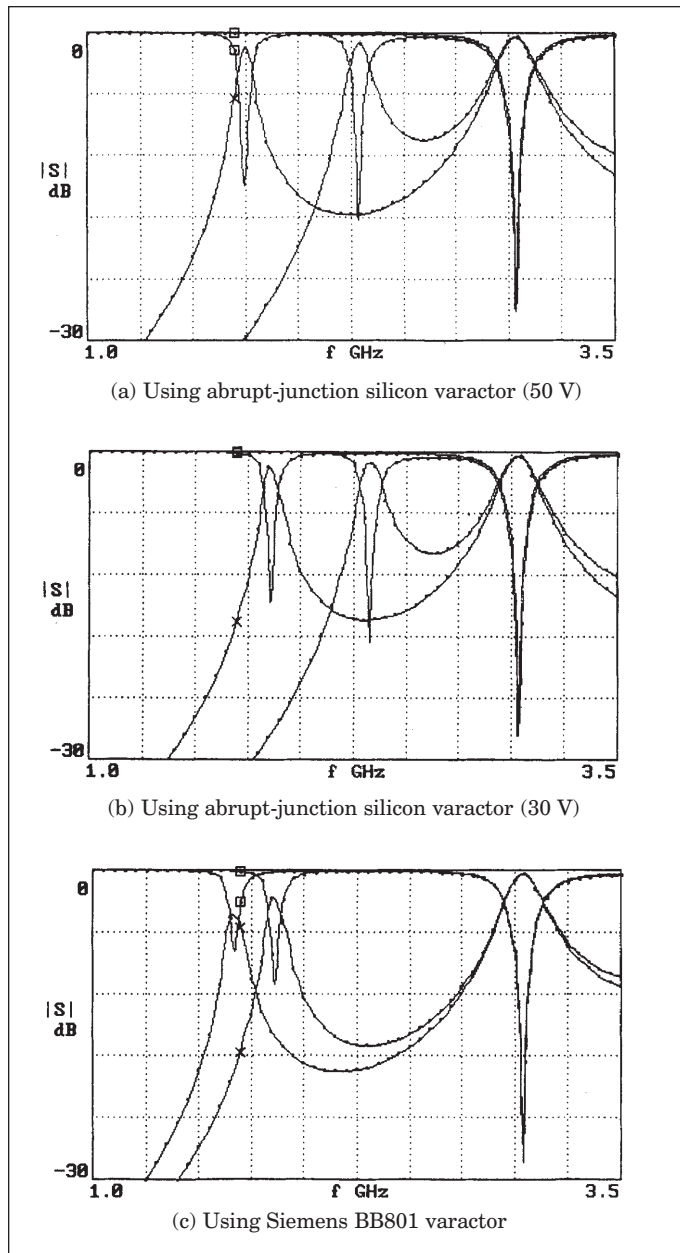
This article describes the exact circuit models for both single and double terminated varactor tuned resonators (VTRs) in MIC realization. Based on such models, resonance conditions and tuning range of the configurations discussed are calculated. Using the computer simulated results, recommendations for practical implementation are given, taking into account real varactor characteristics.

Acknowledgement

This work was supported by INTAS Administration under Project no.96-0851. The authors would like to thank Project Coordinators Dr. B. Jarry (IRCOM, France) and Dr. M. Guglielmi (ESA ESTEC, The Netherlands) for current discussions and supporting the topics considered. ■

References

1. B. Yu. Kapilevich, Abd. Rahman Tharek and Abd. Ghani Kamarruddin, "Modeling Microwave Active



■ **Figure 10. VTM performance for various types of varactor diodes, using capacitive coupling.**

Filters for Mobile Communication System,” *Asia-Pacific Microwave Conf.*, 1995, Korea, Vol. 2, pp. 816-819.

2. S. R. Chandler, I. C. Hunter and J. G. Gardiner, “Active Varactor Tunable Bandpass Filter,” *IEEE Microwave and Guided Wave Letters*, Vol. 3, no. 3,

March 1993, pp. 70-71.

3. I. C. Hunter, J. D. Rodes, “Electronically Tunable Microwave Bandpass Filters,” *IEEE Trans. on MTT*, Vol. 30, no. 9, September 1982, pp. 1354-1367.

4. S. Toyoda, “Quarter-wavelength Coupled Variable Bandstop and Bandpass Filters Using Varactor Diodes,” *IEEE Trans. on MTT*, Vol. 30, no. 9, September 1982, pp. 1387-1389.

5. B. Yu. Kapilevich, “Variety of Approaches to Designing Microwave Active Filters,” *Proc. 27th European Microwave Conf.*, Jerusalem, Vol. 1, 1997, pp. 397-403.

6. B. Yu. Kapilevich, “Understand the Operation of Channelized Active Filters,” *Microwaves & RF*, January, 1997, pp. 89-92.

7. Kai Chang, *Microwave Solid-State Circuits and Applications*, John Wiley & Sons, Inc., 1994.

Author Information

Boris Kapilevich is a Full Professor of microwaves and RF and head of the department at Siberia State Academy of Telecommunications, Novosibirsk, Russia. He received his MS degree from Tomsk State University in 1965, a Ph.D. in 1969 from Novosibirsk State Technical University, and a Dr.Sc. in 1986 from Moscow Power Energy University.



He has over 30 years experience in analysis, design and implementation of various microwave components and devices for the communication industry. His teaching and research interests are in microwave and RF components for mobile and space communications. Prof. Kapilevich is a senior member of the IEEE. He can be reached at his office by tel: +7-3832-660943, by fax: +7-3832-222581 or by e-mail at: boris@neic.nsk.su.

Roman Lukyanets is a post-graduate student at the Siberia State Academy of Telecommunication, Novosibirsk, Russia and a student member of IEEE. He received his MS degree from Siberia State Academy of Telecommunication in 1996. At the moment he is a Ph.D. student whose research interests are focused in microwave and RF components, including optimization of microwave active filters. He can be reached by e-mail at: roman@neic.nsk.su.

